Angular distributions in dissociative collisions of H_2^+ ions at 400 keV and effects of the vibrational states

D. Nir, A. Weinberg, A. Mann, M. Meron, and S. Gordon
Department of Physics, Technion-Israel Institute of Technology, Haifa, Israel
(Received 1 December 1977)

The angular distributions of H_2^+ fragments produced in dissociative collisions in a gas target were measured using an iris aperture. The various dissociation channels were identified by measuring the two fragments and by checking their time coincidence. We have analyzed the statistical moments of the angular distributions in the various dissociation channels and the dependence of these moments on the pressure of the gas target. This analysis presents experimental evidence for the dependence of the dissociation cross sections on the vibrational states of H_2^+, and yields information on the dissociation process.

I. INTRODUCTION

Recent years have evidenced a growing interest in the investigation of atomic reactions by means of molecular projectiles. The use of a molecular projectile enables one to obtain more information, including details of dissociation processes and of the interaction of the projectile with the target atom or the foil. The measurement of the energy profile and the angular distribution of fragments emerging from a foil have yielded information on the interaction in the foil and after it.[1,2] The measurement of the angular distribution and the energy profile in a dissociative collision of H_2^+ in a gas target in the tens of keV energy region has shown that the dissociation mechanism in this energy region is excitation into dissociative states.[3] This information extends our understanding of the basic atomic processes of charge exchange and dissociation. It also has implications for the applied area of plasma fusion reactors where such processes as charge exchange and scattering of molecular fragments take place.

The angular distribution in the ionization of H_2^+ into two H^+ is the result of the electrostatic repulsion between the fragments after ionization. This phenomenon is called Coulomb explosion and it depends on the intramolecular distance before the collision; this distance is a function of the vibrational state of the molecular ion. A similar phenomenon will occur for any repulsive potential. The study of the angular distribution of the dissociation channel $H_2^+ \rightarrow H^0 + H^+$ will contain information on the dissociation mechanism of this channel and its dependence on the vibrational state of H_2^+. Riviere and Sweetman[4] have already shown that the dissociation cross section is not the same for a H_2^+ beam obtained directly from an accelerator, and a secondary beam obtained from the dissociation of H_3^+. They argued that the difference resulted from the different occupation of the vibrational states in the two beams.

In the present work we show by analysis of the statistical moments of the angular distributions and by determining their dependence on the gas-target pressure, that the dissociation cross sections of the higher-vibrational states are larger than those of the lower ones. The results are in accordance with the assumption that the mechanism of the dissociation process is excitation into a dissociative state. We will also compare the results with theoretical calculations based on the Born approximation[5] and with the analytic expression for the dissociation cross section in Gryzinski's theory.[6] The theoretical calculations are able to reproduce only some of the many aspects of the dissociation process.

II. EXPERIMENTAL SYSTEM

A H_2^+ beam at 400 keV was obtained from a Van de Graaff accelerator. The beam was analyzed magnetically, resulting in a clean H_2^+ beam with an energy defined to within a few keV. The percentage of H^+ in the beam was about 1%. The beam's diameter was less than 1 mm and its determination is described below. The beam passed through a cylindrical dissociation chamber, whose length and diameter were both 5 cm (see Fig. 1). The system is similar to a previous one (cf. Ref. 7), with several improvements in the dissociation chamber, which could be rotated and elevated. The diameter of the entrance aperture was 1 mm and that of the exit aperture was 3 mm. The optimal direction for the dissociation chamber was chosen empirically by rotating it to both sides and determining the angle at which the beam does not reach the detector. By this measurement it was determined that the apertures were almost concentric with a deviation of only 0.2 mm. Geometrical considerations show that 98% of the

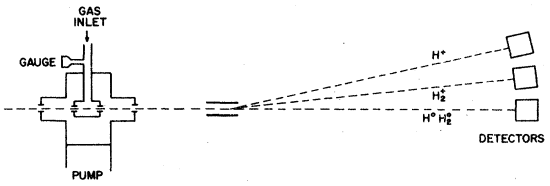

FIG. 1. Schematic description of the experimental system.

dissociation fragments can come out at angles up to 0.9°.

The target gas was air at pressures in the range 5–35 μm, measured directly in the dissociation chamber by a thermocouple gauge. The ratio of pressures in the dissociation chamber and in the detectors's chamber was 150:1.

The dissociated fragments and the undissociated molecules were separated according to their mass and charge by an electrostatic deflector (see Fig. 1) and counted by three detectors at the appropriate angles. The distance of the detectors from the dissociation chamber was 810 mm and their spacing was 30 mm. The detectors were Si surface barrier detectors. Those of the fragments had an active area of 300 mm^2 and those of the undissociated molecules had an active area of 50 mm^2. The latter had a collimator 6 mm in diameter. One of the fragments detectors(according to the needs of the experiment) had a collimator 19 mm in diameter, whereas the other had on it an iris aperture with a variable diameter controlled from outside.

The accurate 0° direction (the beams direction) was determined empirically as the direction at which maximum counts of H_2^+ were obtained at the neutral fragments detector with an iris aperture set to 0.7 mm, while the dissociation chamber was emptied of air and the deflection voltage was set to zero. By this method we also measured the height of the iris center with respect to the incoming beam. The height of the H^+ detector was also checked by deflecting a beam of undissociated ions into this detector (doubling the deflection voltage). Closing the iris aperture to 1 mm did not lower the number of counts. We also measured the minimal and maximal voltage at which undissociated ions entered the H^+ detector with an almost closed iris, and it was estimated that the diameter of the incoming beam is less than 1 mm. We had checked the ratio of counts at the peaks $2H^+/H^+$ (the ratio of counts of proton pairs and single protons) and H_2^+/H^0 (the ratio of counts of molecules at their detector and the counts of a single neutral fragment at the appropriate detector) as a function of the deflection voltage with an open iris. This check showed that all the molecules and their fragments enter the appropriate detector.[7] The deflection voltage for the experiment was set at the point in which the ratio $2H^+/H^+$ was maximal (the ionization channel has the broadest angular distribution, and losing one fragment enlarges the denominator).

The integral angular distribution was measured by counting the number of fragments at a certain dissociation channel as a function of the opening of the iris. The differential angular distribution was evaluated by substraction. The calibration of the iris, namely, determining its diameter as a function of the scale outside of the chamber, was carried out several times during the experiment. There were only small differences between different calibrations and an almost linear relationship between the iris diameter and the external scale. The calibration used for calculations was the one measured at the nearest time or an average of two measurements.

Figure 2 shows the spectrum obtained at the charged-fragments detector H^+. There are two peaks: the higher-energy one (denoted $2H^+$) appears at the energy of the incoming molecule and is obtained from a simultaneous count of two molecular fragments. Therefore it characterizes the ionization channel $H_2^+ \rightarrow H^+ + H^+$. The lower-energy peak appears at half the incoming energy and therefore it corresponds to the count of only one fragment at the detector. Similarly we obtained two peaks

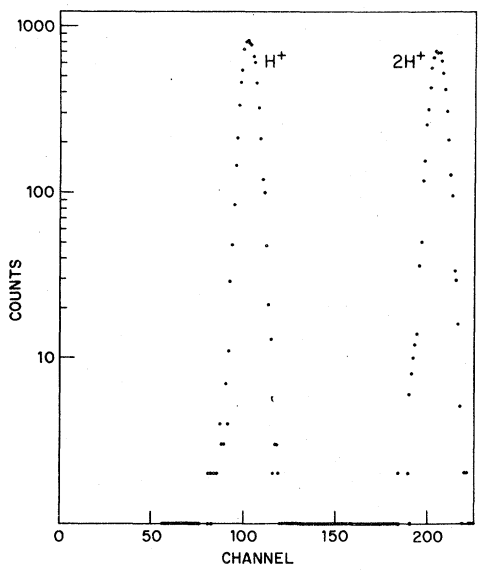

FIG. 2. Spectrum obtained at the charged fragments detector H^+. Two peaks are observed; the lower-energy one arises from a detection of a single H^+ and is denoted H^+; the higher-energy peak arises from the simultaneous detection of two protons (i.e., usually fragments of the same molecule) and is denoted $2H^+$.

TABLE I. Summary of the experimental conditions for measuring the angular distributions of H_2^+ fragments dissociated in air. The particles whose angular distribution was not measured are in parentheses.

No.	Dissociation channel	Iris on detector	Coincidence H^0 and H^+	Normalized to peak
I	$H_2^+ \rightarrow 2H^+$	H^+	no	H_2^+
II	$H_2^+ \rightarrow (H^0)H^+$	H^+	yes	H_2^+
III	$H_2^+ \rightarrow H^0(H^+)$	H^0	yes	H_2^+ or $2H^+$

at the neutral-fragments detector (although the number of $2H^0$ is much smaller than those of H^0). All the results were normalized to the number of undissociated H_2^+ counted in the appropriate detector.

Further coincidence conditions were set in order to characterize the dissociation channel $H_2^+ \rightarrow H^0 + H^+$ (denoted H^0H^+), as described below. Three experimental setups were used in order to measure the angular distributions of all the fragments and they are summarized in Table I. The parameters characterizing each experiment are the location of the iris and the coincidence conditions.

Figure 3 shows the electronic setup for measuring the angular distribution of the ionization channel $H_2^+ \rightarrow 2H^+$ (first row in Table I). The counts of the H^+ detector enter the multichannel analyzer (MCA) whereas those of the undissociated H_2^+ enter a fast scaler, both operated from the control system of the MCA. The detector of the neutral fragments was not used in this setup, as the two H^+ fragments enter the same detector.

Figure 4 shows the electronic setup for measuring the dissociation channel $H_2^+ \rightarrow H^0H^+$ by measuring the angular distribution of the H^+ fragments (second row of Table I). The signals from the H^+ and the H^0 detectors entered a slow coincidence circuit serving as a gate to the MCA. The MCA counts the signal from the H^+ detector, whereas a fast scaler counts the undissociated molecules.

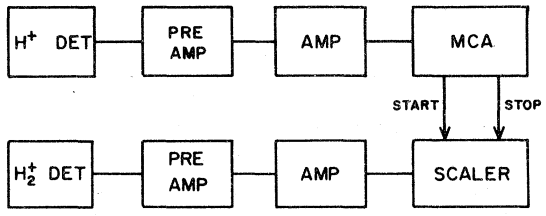

FIG. 3. Electronic system for measuring the ionization channel $H_2^+ \rightarrow 2H^+$. The H^+ fragments are counted in the MCA and the undissociated H_2^+ ions are counted in a fast scaler.

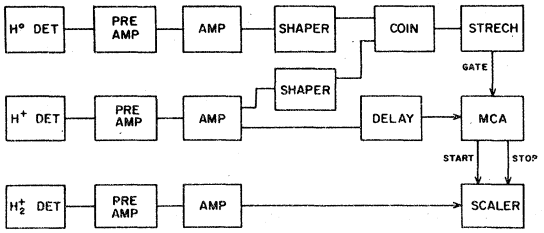

FIG. 4. Electronic system for measuring the dissociation channel $H_2^+ \rightarrow H^0H^+$ by measuring the angular distribution of H^+. The coincidence condition with the neutral fragment is checked and the coincidence signal serves as a gate to the MCA.

The quality of the coincidence was checked by the ratio of the two peaks in the MCA $2H^+/H^+$ measured both under and free of coincidence conditions with the H^0 detector. It was found that 98.5% of the $2H^+$ events were eliminated by the coincidence condition.

Figure 5 shows the electronic setup for measuring the dissociation channel $H_2^+ \rightarrow H^0H^+$ by measuring the angular distribution of H^0 (third row of Table I). The signals from the two fragments detectors were fed in parallel into a coincidence unit and a summing amplifier. The signal from the coincidence unit served as a gate to the sum signal which entered the MCA. The counts were normalized to the counts of undissociated H_2^+ ions in the appropriate detector or sometimes to the counts of the $2H^+$ in the charged particles detector. This complicated arrangement enabled a better check of the quality of the coincidence. The sum peak H^0H^+ appears at different channels in the MCA than those of H^+ and $2H^+$, and therefore the remaining spurious counts after the coincidence (1.5%) are not added to the true ones. It should be emphasized that the coincidence condition between the two detectors from the H^0H^+ dissociation channel is the most efficient one in reducing the background from single detector events

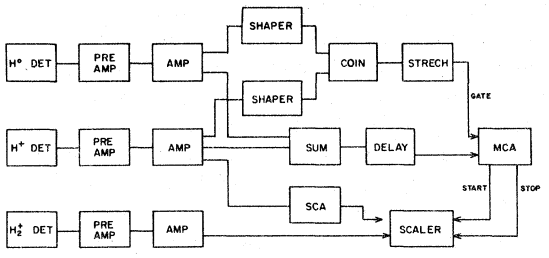

FIG. 5. Electronic system for measuring the dissociation channel $H_2^+ \rightarrow H^0H^+$ by determining the angular distribution of H^0. The coincidence condition with the charged fragment is checked and the coincidence signal serves as a gate to the sum signal in the MCA.

as $2H^+$ and $2H^0$ dissociation channels and H^0 and H^+ single particles which come with the beam.

III. EXPERIMENTAL RESULTS AND ANALYSIS

A. Method of analysis

In this experiment we measured the integral angular distribution of the dissociation fragments in each dissociation channel as a function of the diameter of the iris aperture. As described above, the ionization channel is given by the peak denoted $2H^+$ in the spectrum of the charged fragments detector, having the full projectile energy. The dissociation channel H^0H^+ was separated by a coincidence condition of the two fragment detectors from the single proton arriving with the beam.

The integral angular distribution is evaluated directly from the ratio between the number of counts in a dissociation channel and the number of undissociated molecules. The distribution was arbitrarily normalized to 1.0 for an open iris (0.7°). The differential angular distribution was calculated by a subtraction of two nearby measurements of the integral distribution. For the ionization channel, the differential angular distribution is explicitly written with its error:

$$f_{2H^+}\left(\frac{\theta_1+\theta_2}{2}\right)=\left[\left(\frac{2H^+}{H_2^+}\right)_0\left(\frac{\theta_1+\theta_2}{2}\right)(\theta_1-\theta_2)\right]^{-1}\left\{\left[\left(\frac{2H^+}{H_2^+}\right)_1-\left(\frac{2H^+}{H_2^+}\right)_2\right]\right.$$
$$\left.\pm\left[\left(\frac{1}{H_2^+}+\frac{1}{2H^+}\right)_1\left(\frac{2H^+}{H_2^+}\right)_1^2+\left(\frac{1}{H_2^+}+\frac{1}{2H^+}\right)_2\left(\frac{2H^+}{H_2^+}\right)_2^2\right]^{1/2}\right\}. \quad (1)$$

Here, 1 and 2 denote the two measurements, θ_1 and θ_2 the opening angles of the iris, H_2^+ and $2H^+$ are the number of counts in the appropriate peaks, and $(2H^+/H_2^+)_0$ is the ratio for a completely open iris. The calculated error includes only the statistical error. It is about 3% and is the dominant one. In atomic-hydrogen beams, H^0 and H^+ charge exchange is almost entirely unidirectional ($H^0 \rightarrow H^+$) in this energy range. In a H_2^+ beam in this energy range the probability of ionization is two times larger than dissociation.[7] An addition of a few percent of spurious counts coming from the H^0H^+ channel to the $2H^+$ channel will not change its angular distribution, whereas the H^0H^+ angular distribution is not affected due to the direction of the charge-exchange process.

The fraction of dissociation was obtained from two complementary measurements: the signal from the neutral fragments detector being in coincidence and in anticoincidence condition with the signal from the H^+ detector. (The counts were normalized to the number of undissociated ions.)

$$D=\left[\left(\frac{2H^+}{H_2^+}\right)+\left(\frac{H^0H^+}{H_2^+}\right)\right]\Big/\left[\left(\frac{2H^+}{H_2^+}\right)+\left(\frac{H^0H^+}{H_2^+}\right)+1\right]. \quad (2)$$

The nth-order statistical moment of the experimental angular distribution and its error were calculated by the following expression [δf is the experimental error given in eq. (1)]:

$$\overline{\theta^n}=\sum_{\theta i=0}^{\theta_{max}}\theta_i^{n+1}f(\theta_i)\Delta\theta_i \pm\left(\sum_{\theta i=0}^{\theta_{max}}[\theta_i^{n+1}\delta f(\theta_i)\Delta\theta_i]^2\right)^{1/2}. \quad (3)$$

The index i runs over the measured points, and the sum was truncated at θ_{max}. θ_{max} is the angle at which the value of the angular distribution was (2–3)% of its maximal value. We calculated the moments of order 0, 1, 2, 4 and their errors. Further reduction of the errors was achieved by calculating the ratios between the moments which are less sensitive to all kinds of errors. This is due to the numerator and denominator being quantities of positive correlation. The coefficient of linear correlation between the errors of the various moments was calculated and was found to be larger than 90%. A derivation of an analytical expression of the error in the ratio of the moments is not simple. The problem was circumvented by preparing sets of pseudorandom numbers which represented the errors in the values of the various $f(\theta_i)$. For several dozens of these sets we checked the propagation of the error in each of the moments separately and in their ratios. It was found that the probable error in the ratios $\overline{\theta^1}/\overline{\theta^0}$, $\overline{\theta^2}/\overline{\theta^1}$, $\overline{\theta^4}/\overline{\theta^2}$ is smaller by a factor of 2–3 than the probable error in the higher moment, both for random numbers with equal probability in the interval [0, 1] and for random numbers with a larger probability near 0. The error shown in the figures (and used in the calculations) for the ratio of the moments is one-half of the probable error of the higher moment, computed according to Eq. (3). We usually have about 12 points in the angular distribution. It follows that there is a total reduction of the random error in the ratios of the moments by a factor of about $2\sqrt{12}$, and also a

large reduction of systematic errors, such as variations in pressure, variation in the accelerator parameters, or variation in the counting rate. We can therefore observe effects which are not large. In order to obtain overlapping data from the various moments, the ratios of the various moments in the ionization channel were multiplied by constant factors. The constant factor for each couple of moments was obtained by using the moments of the angular step distribution (which is a reasonable approximation to the experimental distribution). These moments satisfy

$$\bar{\theta}^n_{2H^+} = [1/(n+2)]\theta^{n+2}_{max} . \quad (4)$$

In the dissociation channel H^0H^+ the angular distribution is different, and the multiplication factor was calculated for each couple of moments by using an angular distribution proportional to $\theta^{-1/2}$, which satisfies

$$\bar{\theta}^n_{H^0H^+} = [1/(n+1.5)]\theta^{n+1.5}_{max} . \quad (5)$$

The data, overlapping $\bar{\theta}^1/\bar{\theta}^0$, was plotted versus the dissociation fraction D.

B. Results

The differential angular distributions of the dissociation channels were calculated from the integral ones by the method described above, and the results are presented in Fig. 6. The H_2^+ energy is 400 keV, and the dissociation channel and the dissociation fraction are shown in the figure. The particles in the dissociation channel whose angular distribution was not measured appear in parentheses. In the channel $H_2^+ \rightarrow 2H^+$, we see clearly the distribution resulting from the Coulomb explosion;

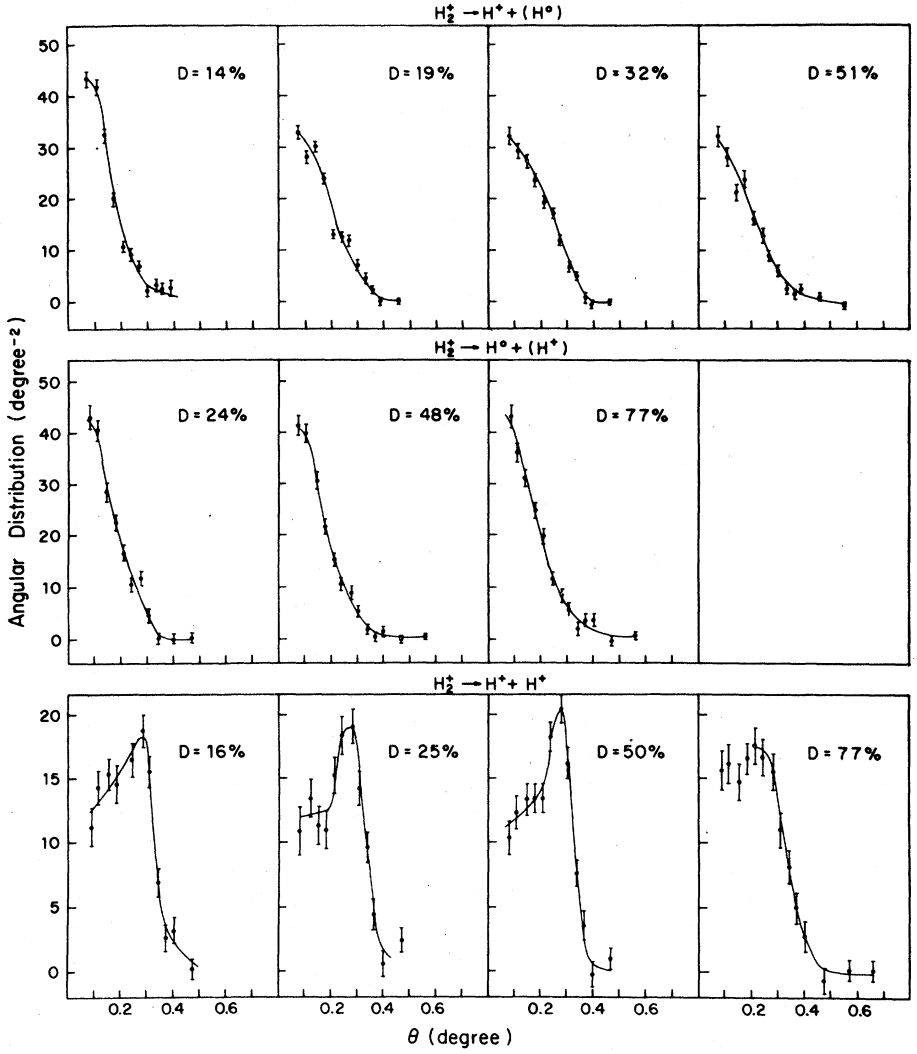

FIG. 6. Summary of the measurements of the angular distribution in the two dissociation channels. In each plot we indicate the dissociation channel, the detected particle, and the dissociation percentage D. $H_2^+ \rightarrow H^0(H^+)$ means measurement of the angular distribution of H^0 in the H^0H^+ channel, etc. The H_2^+ energy is 400 keV and the pressure in the dissociation chamber 10–30 μm.

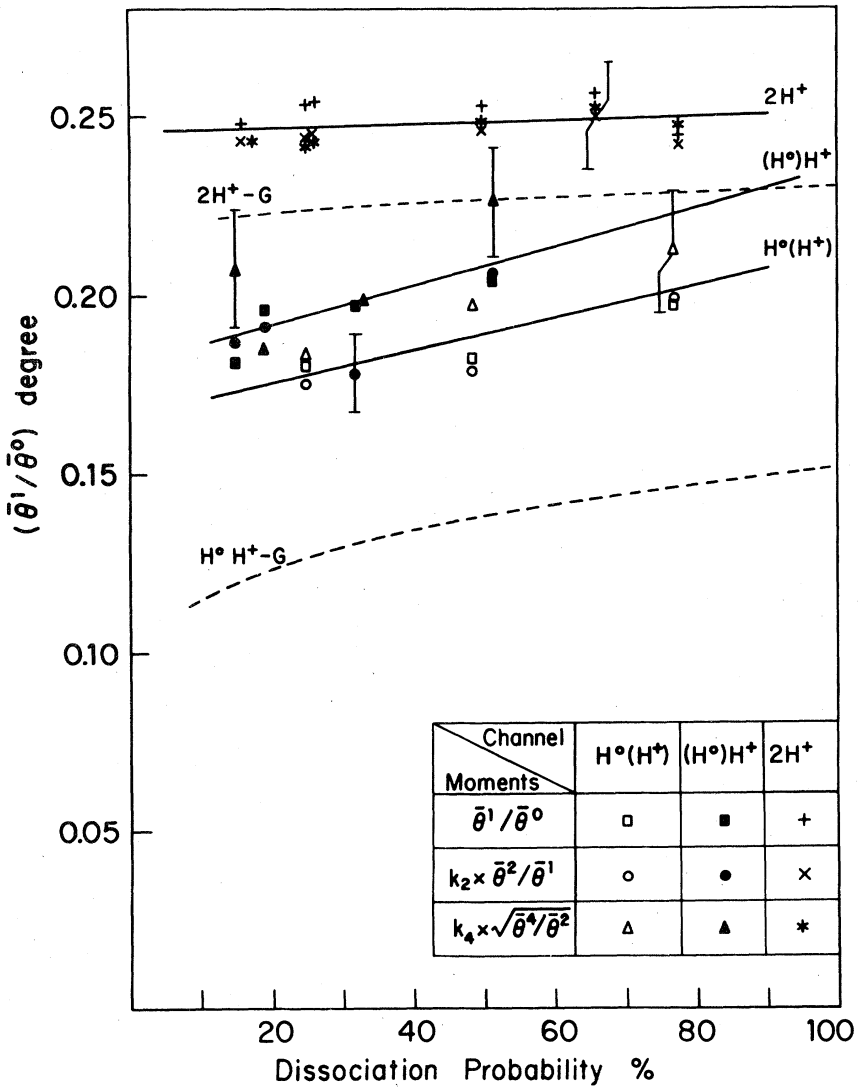

FIG. 7. Dependence of the ratios of the statistical moments of the angular distribution (see text) in the various channels on the dissociation probability. The channels are indicated near the solid lines which are the lines of linear regression of the experimental points. Particles whose angular distribution was not measured are in parentheses. The ratios of the higher moments are scaled to the value of θ^1/θ^0 as described in the text (for the identification of these moments, see table in the figure). The dashed lines denoted by G and by the appropriate dissociation channel are the theoretical predictions using the Gryzinski formula (see text).

at an angle of about 0.28° there is a maximum whose position is insensitive to changes in the pressure. The angular distributions in the H^0H^+ channel which were measured for both H^0 and H^+ are very similar and in general they broaden with an increase in the pressure.

Figure 7 shows the ratios of the various moments (corrected as described above), plotted versus the total dissociation fraction. The ratios of moments yielded a large amount of independent data, whereas the systematic and the random errors were reduced. The corrected ratios of the various moments are indicated in the figure by different characters, and the dissociation channels are also indicated. $\bar{\theta}^1/\bar{\theta}^0$ in the $2H^+$ channel rises very slowly, whereas in the H^0H^+ channel there is a large increase in $\bar{\theta}^1/\bar{\theta}^0$ of the neutral fragments H^0 (H^+), and a similar increase for the protons H^+ (H^0). The dashed lines and the G denote the theoretical calculations of the moments by a formula of Gryzinski[6] as described below.

IV. DISCUSSION AND COMPARISON WITH THEORY

A. Discussion of the results

In the channel $H_2^+ \rightarrow 2H^+$ the loss of the electron results in electrostatic repulsion between the two fragments. There is a minimum in the angular distribution at $\theta = 0$ (Fig. 6) and a maximum at $\theta \sim (E_c/E)^{1/2}$ (E_c is the repulsion energy of the two protons in the molecule). This phenomenon is called Coulomb explosion and its cause is transfer of internal potential energy into kinetic energy of the fragments.[1,2] The phenomenon was investigated and the corresponding angular distribution is known.[1,2] In the other dissociation channel, $H_2^+ \rightarrow H^0H^+$, the electron is excited from the $1S\sigma g$ level into the $2P\sigma u$ level which is dissociative;

the fragments repel one another and the molecule dissociates into a hydrogen atom and a proton.[3] The angular distribution is similar to that of the $2H^+$ channel, but it is narrower[3] due to a smaller potential energy in the center-of-mass system.[8] Using the functional form of the angular distribution of the Coulomb explosion,[1] we obtain an expression for the angular distribution in a dissociation channel as a sum over the various vibrational states of H_2^+:

$$f(\theta)=\sum_{v=0}^{v_{\max}} P_v\left(\frac{\sigma_v}{\sigma_{T,v}}\right)(1-e^{-\sigma_{T,v}N}) \times\left(\frac{E_v}{E}\right)^{-1}\left[1-\left(\frac{E_v}{E}\right)^{-1}\theta^2\right]^{-1/2}. \quad (6)$$

Here v denotes the vibrational state and P_v its occupation probability, calculated according to the Franck-Condon principle.[9] E_v is the potential energy transformed into kinetic energy after excitation or ionization (for the dissociation channel H^0H^+, $E_v=E^*_{2P\sigma u}-E_\infty$). E is the kinetic energy of the molecule in the laboratory system and θ the scattering angle in that system. $\sigma_{T,v}$ is the total dissociation cross section of H_2^+ in the vibrational state v, and N is the number of scatterers per unit area; hence $1-e^{-\sigma_{T,v}N}$ is the fraction of dissociated molecules. N is pressure dependent and $\sigma_{T,v}$ may be different for each vibrational state, therefore the fraction of dissociated molecules changes with the vibrational state and pressure. The fraction that goes into a specific channel is $\sigma_v/\sigma_{T,v}$ (σ_v is the cross section for dissociation into this specific channel). The statistical moments of the angular distribution are given by

$$\bar{\theta}^n=\int_0^\pi \theta^n f(\theta)\sin\theta\, d\theta. \quad (7)$$

Since $f(\theta)$ vanishes rather fast, there is no contribution from large angles and $\sin\theta$ may be replaced by θ. Changing variables: $(E_v/E)^{-1/2}\theta=\sin\alpha$ we obtain

$$\bar{\theta}^n=\sum_{v=0}^{v_{\max}} P_v\left(\frac{\sigma_v}{\sigma_{Tv}}\right)(1-e^{-\sigma_{T,v}N}) \times\left(\frac{E_v}{E}\right)^{n/2}\int_0^{\pi/2}\sin^{n+1}\alpha\, d\alpha. \quad (8)$$

The integral

$$I_n=\int_0^{\pi/2}\sin^{n+1}\alpha\, d\alpha$$

is easy to solve: $I_0=1$, $I_1=\frac{1}{4}\pi$, $I_2=\frac{2}{3}$, $I_4=\frac{8}{15}$. From the expression for the moments of $f(\theta)$ [Eq. (8)] we may reach certain conclusions about the dissociation processes and compare them with theoretical predictions. As E_v and P_v are known[8,9], we can use the moments to check theories for σ_v. Three types of expressions were checked: (a) $\sigma_v=\sigma$ independent of the vibrational state; (b) σ_v at $E_{H_2^+}=400$ keV was taken as proportional to σ_v calculated by Berkner *et al.*[5] in the Born approximation at $E_{H_2^+}=20$ MeV. In this approximation the dominant energy dependence is through a factor E^{-1} yielding a multiplicative factor. A rather mild energy dependence entering through the change of the integration limits was not taken into account. (c) σ_v is taken from the corresponding analytical expression of Gryzinski [Ref. 6, Eq. (29)]:

$$\sigma_v=\frac{2\pi(q_1q_2)^2}{U^2E_2}\left(U+\tfrac{2}{3}E_1\right), \quad E_2\geq E_1+U. \quad (9)$$

Here $E_2=(m_e/2m_p)E_{H_2^+}$, E_1 is the kinetic energy of a target electron, and U is the minimum ionization energy. For N_2 the energy of a $2s$ electron is 10.3 eV and that of a $2p$ electron is 6.1 eV (see Ref. 5); hence $\bar{E}_1=7.8$ eV. [In the formula an expression whose order of magnitude is $U/(E_2-E_1)$ which is much less than 1 for our projectile energy, was neglected.]

The number of scatterers per unit area, N, may be deduced from the pressure measured by a thermocouple in the dissociation chamber. However we preferred to take several values for N and to calculate the moments for each of them. The proper value of N was chosen as the one reproducing the sum $D=\bar{\theta}^0_{H^0H^+}+\bar{\theta}^0_{2H^+}$ which gives the total dissociation.

If $\sigma_{T,v}=\sigma$ (cross-section independent of the vibrational state), it follows that the ratios of the statistical moments of the angular distribution should be independent of the gas pressure. The increase of the ratios of the moments in the H^0H^+ channel with increasing pressure shows that the cross section rises with the vibrational state. The possibility that the increase is due to multiple scattering is ruled out because the average number of collisions $(1-D)^{-1}$ is between 1 and 4 in our case. The similarity between the angular distributions of the protons $f_{(H^0)H^+}$ and of the neutral fragments $f_{H^0(H^+)}$ in the H^0H^+ channel shows that the internal energy is equally divided between the two fragments, conforming to the model of excitation to a dissociative state. The physical significance of the effect which broadens somewhat the angular distribution of H^+ compared with that of H^0 is not clear. Because the systems measuring the distributions are different and the iris is mounted on a different detector, we cannot exclude the possibility of a systematic experimental error.

The dependence of the moments on the percentage of dissociation is different in the $2H^+$ and H^0H^+

TABLE II. Comparison of experimental results with various theoretical predictions (see also Fig. 7). The first row of the table compares charge-state probabilities. The rest of the table contains comparisons of the ratio of moments $\bar{\theta}^1/\bar{\theta}^0$ and its D dependence.

Quantity compared	Experimental result	Result assuming σ_v independent of v	Gryzinski's theory	Born approximation
[(probability of H^0H^+)/(probability of $2H^+$)] at $D=20\%$	0.82 (taken from Ref. 7)	...	3.30	0.60
Slope of linear regression of the $H^0(H^+)$ channel	0.044	0	0.034	0.005
Ordinate of the regression line of $H^0(H^+)$ at $D=25\%$	0.178	0.153	0.127	0.146
Slope of linear regression of the $(H^0)H^+$ channel	0.053	0	0.034	0.005
Ordinate of the regression line of $(H^0)H^+$ at $D=25\%$	0.194	0.153	0.127	0.146
Slope of the linear regression line of the $2H^+$ channel	0.004	0	0.007	0.002
Ordinate of the regression line of $2H^+$ at $D=25\%$	0.247	0.226	0.224	0.225

channels. This difference cannot be attributed to any experimental cause, and it supports the conclusion that the dissociation cross section increases with the vibrational state. If σ_v depends on the vibrational state, the moments of the two channels will show different trends. This is further enhanced by the fact that the dependence of E_v on the initial vibrational states is quite different in the two channels. E_v in the ionization channel changes by a factor of 2 between the lowest and highest vibrational states, whereas in the H^0 H^+ channel E_v changes by a factor of 10 and more (see figure in Ref. 8).

A quantitative comparison with the various calculations is shown in Table II. The characteristic values chosen for comparison are (i) the ratio of probabilities of the different channels (charge states of pairs); (ii) the ratio of moments $\bar{\theta}^1/\bar{\theta}^0$ at 25% dissociation; (iii) the slope of the linear regression curve of the ratio of moments $\bar{\theta}^1/\bar{\theta}^0$ vs D. The feature common to all the calculations is that the theoretical value of the ratio of moments is lower than the value derived from the experimental angular distribution. In the $2H^+$ channel it is 0.23° as compared with 0.25°, and in the H^0H^+ channel 0.11° – 0.14° as compared with 0.18° – 0.21°. This is probably caused by the dissociation-chamber entrance aperture having a diameter of 1 mm which is equivalent to 0.07°. The differences in broadening in the various channels reside in the form of the angular distribution. It is not clear how to take this broadening into account, and therefore we preferred to compare the results with the theory without any corrections.

Assuming that the cross sections are proportional to the cross section calculated by the Born approximation at 20 MeV yields a ratio between the charge states of the various channels which is near the experimental value. But in each channel there is no dependence on the gas pressure and on the dissociation fraction. Use of Eq. (9), which is an analytic expression from Gryzinski's theory for our energy range, shows effects of dependence on the gas pressure. In the $2H^+$ channel the theoretically expected increase in the ratio of moments is very small (as is also obtained experimentally). For the H^0H^+ channel, calcula-

tions using cross sections based on Eq. (9) predict a monotonic increase in the ratio of moments with the dissociation fraction. At high D the ratio of moments is 30% more than at low D. Approximations in Eq. (9) (such as $E_1 \gg U$ or $E_1 \ll U$) change the moments by approximately 10%. However, the Gryzinski formula in (9) does not reproduce the experimental charge states (it predicts that H^0H^+ is three times more probable than $2H^+$). This discrepancy stems from the very nature of Eq. (9) because the excitation energy into the dissociation channel H^0H^+ is always lower than that of the ionization channel $2H^+$. Therefore Gryzinski's theory does not describe properly the dissociation of H_2^+, and one has to postulate either additional contributions to the ionization channel $2H^+$ which increase its cross section or some constraints on the dissociation channel H^0H^+ which diminish its cross section. Indeed, various corrections, such as adding a constant term to the ionization cross section or lowering the H^0H^+ cross section by a factor of 3 yield reasonable agreement with the angular distribution and the charge states. The experimental data, however, do not tell us the necessary modification of the theory.

Figure (7) shows also the comparison with Gryzinski's theory without corrections to the cross sections in Eq. (9). The dashed lines describe the statistical moments of the angular distributions. The ratio of the measured moments is larger than the calculated ones (probably due to the finite widths of the apertures), but the calculated dependence on the gas pressure is similar to the experimental one.

V. SUMMARY AND CONCLUSIONS

Several interesting phenomena were exhibited in the charge states and in the statistical moments of the angular distributions of the H_2^+ fragments. The probabilities of the charge states are almost equal in the two channels. The statistical moments of the angular distribution in the $2H^+$ channel is almost independent of the gas pressure; in the H^0H^+ channel they increase with the pressure. Checking the theories, it turned out that the moments of the angular distribution depend significantly on the pressure only when there are large differences in the cross sections for the various vibrational states [such as in (9)]. However, a dependence of the cross sections on the excitation energy as in (9) yields a wrong prediction of the charge states.

ACKNOWLEDGMENTS

We are grateful to Professor B. Rosner for very helpful suggestions, to Miss Pirjo Putila for her help in the experiments and the calculations, and to J. Saban and J. Shlomi for their help.

[1] J. Golovchenko and E. Laegsgaard, Phys. Rev. A 9, 1215 (1974).
[2] D. S. Gemmel and Z. Vager, Phys. Rev. Lett. 34, 1420 (1975); 37, 1352 (1976); Phys. Rev. A 14, 638 (1976).
[3] B. Meierjohann and M. Vogler, J. Phys. B 9, 1801 (1976); Z. Phys. A 282, 7 (1977); H. S. W. Massey, E. H. S. Burhop, and H. B. Gilbody, *Electronic and Ionic Impact Phenomena* (Oxford University, London, 1974), Vol. 4.
[4] A. L. Riviere and D. R. Sweetman, Proc. Phys. Soc. 78, 1215 (1961).
[5] K. H. Berkner, S. N. Kaplan, R. V. Pyle, and J. W. Stearns, Phys. Rev. 146, 9 (1966).
[6] M. Gryzinski, Phys. Rev. 138, A323 (1965); 138, A336 (1965).
[7] D. Nir, B. Rosner, A. Mann, and D. Maor, Phys. Rev. A 16, 1483 (1977).
[8] T. E. Sharp, At. Data 2, 119 (1971); G. Hunter, A. W. Yan, and H. O. Pritchard, At. Data Nucl. Data Tables 14, 11 (1974).
[9] W. L. Walters, D. G. Costello, J. G. Skofronick, D. W. Palmer, W. E. Kane, and R. G. Herb, Phys. Rev. 125, 2012 (1962); W. Brandt and R. H. Ritchie, Nucl. Instrum. Meth. 132, 43 (1976).